

Magnetization and susceptibility of the Kondo compounds $\text{CeCu}_{5-x}\text{Al}_x$, $x = 0, 1, 1.5, 2$

This article has been downloaded from IOPscience. Please scroll down to see the full text article.

1998 J. Phys.: Condens. Matter 10 4465

(<http://iopscience.iop.org/0953-8984/10/20/014>)

View [the table of contents for this issue](#), or go to the [journal homepage](#) for more

Download details:

IP Address: 171.66.16.209

The article was downloaded on 14/05/2010 at 16:22

Please note that [terms and conditions apply](#).

Magnetization and susceptibility of the Kondo compounds CeCu_{5-x}Al_x, $x = 0, 1, 1.5, 2$

E Bauer[†], G Amoretti[‡], L C Andreani[§], B Delley^{||}, M Ellerby[¶],
K McEwen[¶], R Monnier⁺, E Pavarini^{*‡} and P Santini^{*}

[†] Institut für Experimentalphysik, Technische Universität Wien, A-1040 Wien, Austria

[‡] Istituto Nazionale per la Fisica della Materia, Dipartimento di Fisica, Università di Parma, I-43100 Parma, Italy

[§] Istituto Nazionale per la Fisica della Materia, Dipartimento di Fisica 'A Volta', Università di Pavia, I-27100 Pavia, Italy

^{||} Paul Scherrer Institut, CH-5232 Villigen PSI, Switzerland

[¶] University College London, Department of Physics and Astronomy, London WC1E 6BT, UK

⁺ Laboratorium für Festkörperphysik, ETH-Hönggerberg, CH-8093 Zürich, Switzerland

^{*} Institut de Physique Théorique, Université de Lausanne, CH-1015 Lausanne, Switzerland

Received 2 December 1997

Abstract. Various magnetic measurements on CeCu_{5-x}Al_x, $x = 0, 1, 1.5, 2$, indicate that increasing Kondo interaction due to Cu/Al substitution causes a substantial decrease of the magnetic moment in the crystal-field ground state. A theoretical description on the basis of the non-crossing approximation, taking into account the primary interaction mechanisms, yields excellent agreement with the data and shows that the moment is reduced even at high values of applied magnetic field.

1. Introduction

The classical picture of the Kondo effect acting in a particular system involves the quenching of localized magnetic moments owing to a cloud of conduction electrons. Measurements of the moment using isothermal magnetization or elastic neutron scattering reveal that the magnetic moment can be significantly smaller than that expected for a certain crystal-field configuration. Supplying sufficient thermal or magnetic energy to such a system causes a break-up of the singlet ground state, and a consequent destruction of the Kondo state.

The aim of this investigation is to demonstrate that a reduction of the moments due to Kondo interaction persists in high fields, even for those cases where T_K is relatively small. The search for exact solutions of the Kondo problem [1] has been complicated in the case of real materials where the effects of anisotropy, crystal fields (CF) and molecular fields may all coexist. Another feature of the Kondo effect which is addressed here is the influence on the susceptibility at temperatures much larger than the Kondo scale, also in the presence of CF effects. A system which has already been studied in some detail is the hexagonal binary compound CeCu₅ which orders antiferromagnetically (AFM) at $T_N \approx 4$ K [2, 3]. The ordered moment was determined as $0.36 \mu_B$ with the moments aligned ferromagnetically perpendicular to the basal plane, with a modulation vector $\mathbf{q} = [0, 0, 1/2]$ [4]. Theoretically, if the Kondo interaction is omitted, the moments expected for the $|\pm 1/2\rangle$ ground state are

[‡] Present address: Max-Planck-Institut für Festkörperforschung, Heisenbergstrasse 1, D-70569 Stuttgart, Germany.

$0.42 \mu_B$, and a Kondo interaction strength of $T_K \approx 2.2$ K has been evaluated to explain the difference between the observed and theoretical values of the moments.

The physical properties change substantially as a result of substitutions of Al for Cu in CeCu_5 . Such a substitution is possible for at least two Cu atoms without changing the hexagonal crystal structure. However, since the Al/Cu substitution happens almost exclusively at the 3g sites of the CaCu_5 structure, partially disordered alloys $\text{CeCu}_{5-x}\text{Al}_x$ are formed. Furthermore, because the monoelectronic Cu atom is replaced by Al, which usually provides three conduction electrons, a change of the electronic structure is to be expected. Initially, the Al/Cu substitution causes the vanishing of long-range magnetic order and simultaneously the electronic contribution to the specific heat c/T becomes very large, of the order of that of typical heavy-fermion systems [3, 5]. In terms of Kondo interaction, it is obvious that T_K increases due to this substitution and $k_B T_K$ may eventually overcome the RKKY interaction strength. Since long-range magnetic order with reduced magnetic moments is involved, T_K does not scale inversely with c/T . From inelastic neutron scattering experiments it was observed that even the crystal-field level scheme changes drastically as a result of the Al/Cu substitution. Therefore it is necessary to consider the Kondo interaction together with the appropriate CF scheme in order to give a full interpretation of the magnetic behaviour.

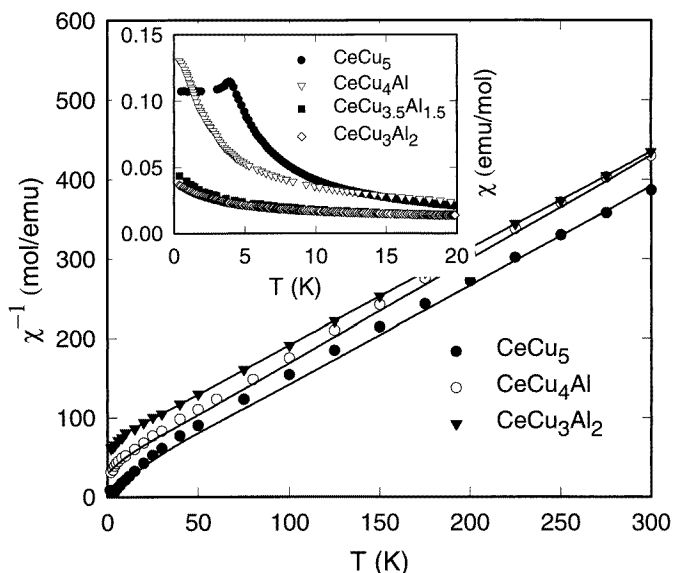


Figure 1. The temperature-dependent magnetic susceptibility χ^{-1} for various concentrations of $\text{CeCu}_{5-x}\text{Al}_x$. The solid lines are least-squares fits to the data. The inset shows $\chi(T)$ at low temperatures.

This paper first presents the experimental studies of the magnetic susceptibility $\chi(T)$ and isothermal magnetization $M(H)$ for selected concentrations of $\text{CeCu}_{5-x}\text{Al}_x$. We then present a theoretical description that models the experimental studies. In order to develop a satisfactory description we develop the theory in two stages. The first stage was to take account of the most important interaction mechanisms present in these alloys, crystalline electric fields and molecular-field effects. The theory is then extended to take into account the Kondo effect, and this is achieved using the self-consistent large-degeneracy expansion

in the non-crossing approximation (NCA). This final stage includes the effects due to crystal fields and molecular fields [6, 7]. Since in general T_K increases with the spin degeneracy, the thermal population of the various crystal-field levels will cause an increase of the effective T_K with temperature, and in turn $\chi(T)$ is influenced even at high temperatures by the Kondo effect.

Significant changes of the main interaction mechanisms in the alloy series provide the possibility of determining various parameters experimentally. Therefore, a theoretical description can be obtained with just a small number of adjustable parameters.

Table 1. Physical properties and parameters used in the calculations for the compounds $\text{CeCu}_{5-x}\text{Al}_x$.

$\text{CeCu}_{5-x}\text{Al}_x$	$x = 0$	$x = 1$	$x = 2$
\mathbf{k}	(0, 0, 1/2)	—	—
T_N (K)	3.95	—	—
μ_{Ce} (μ_B/Ce)	0.36	—	—
μ_{eff} (μ_B/Ce)	2.5	2.37	2.54
θ_p (K)	−20	−28	−40
ΔE_Q (mm s^{-1})	3.4	3.07	2.35
Δ_1 (K)	190	60	60
Δ_2 (K)	603	522	406
B_2^0 (K)	33.6	30.3	23.2
B_4^0 (K)	0.039	0.41	0.27
<i>CF calculation:</i>			
$\lambda_{\parallel}^{\text{para}}$ (mol emu^{-1})	−130	−296	−45
$\lambda_{\perp}^{\text{para}}$ (mol emu^{-1})	0.89	−6	−32
<i>NCA calculation:</i>			
T_K (K)	2.2	5	9.5
$\lambda_{\parallel}^{\text{para}}$ (mol emu^{-1})	0	0	0
$\lambda_{\perp}^{\text{para}}$ (mol emu^{-1})	4.2	−1.8	−14.3
$\lambda_{\parallel}^{\text{ord}}$ (mol emu^{-1})	94.9	—	—
$\lambda_{\perp}^{\text{ord}}$ (mol emu^{-1})	0	—	—

2. Magnetic susceptibility of $\text{CeCu}_{5-x}\text{Al}_x$

The temperature-dependent magnetic susceptibility $\chi(T)$ of $\text{CeCu}_{5-x}\text{Al}_x$ was measured from 0.3 K up to room temperature. The results of these measurements are shown in figure 1. The inset of this figure shows the antiferromagnetic phase transition of CeCu_5 around $T_N \approx 4$ K. Carefully performed specific heat measurements indicate that there is not a single phase transition; rather, two transitions with $T_1 = 3.85$ K and $T_2 = 4.08$ K are present [3, 8]. As mentioned above, the Al/Cu substitution suppresses long-range magnetic order, which is clearly observed in the susceptibility measurements. At high temperatures $\chi^{-1}(T)$ follows a Curie–Weiss behaviour with effective moments close the value of the free Ce^{3+} ion, and thus indicates that the Al/Cu exchange does not drive the system towards an

intermediate-valence state. The paramagnetic Curie temperature θ_p evaluated from least-squares fits of the Curie–Weiss law above 50 K increases from about -20 K to about -40 K as x goes from 0 to 2 (compare table 1).

2.1. Crystal-field-derived susceptibility

The crystal-field Hamiltonian accounting for the hexagonal cerium systems studied (CaCu_5 structure, $P6/mmm$) can be written as

$$H_{CF} = B_2^0 O_2^0 + B_4^0 O_4^0 \quad (1)$$

with B_n^m the crystal-field parameters and O_n^m the Stevens operator equivalents. Since $m = 0$ in each case, there are diagonal matrix elements only, causing that the CF-state doublets to be pure eigenstates $|\pm 1/2\rangle$, $|\pm 3/2\rangle$ and $|\pm 5/2\rangle$. The CF splitting requires the Van Vleck contribution to be taken into account for a description of the magnetic susceptibility over the whole temperature range. If a magnetic field is applied along a certain direction α in the crystal, the magnetic susceptibility is given within the scope of the Van Vleck formula by

$$\chi_\alpha^{CF} = \left[N_A (g_j \mu_B)^2 / \left(\sum_n \exp(-E_n/k_B T) \right) \right] \times \sum_{r,s} |\langle r | J_\alpha | s \rangle|^2 e^{-E_r/k_B T} \frac{\exp((E_r - E_s)/k_B T) - 1}{E_r - E_s}. \quad (2)$$

N_A is the Avogadro number, E_r the energy of the r th state, g_j the Landé g -factor, and $\langle r | J_\alpha | s \rangle$ the matrix element of J_α connecting the r -state and s -state of the respective CF scheme. Usually the c -axis is chosen as the quantization z -direction.

The \mathbf{q} -dependent molecular-field constants are generally defined as

$$\lambda(\mathbf{q}) = \frac{1}{N_A (g \mu_B)^2} \sum_{\mathbf{R} \neq 0} J(\mathbf{R}) e^{i\mathbf{q} \cdot \mathbf{R}} \quad (3)$$

where $J(\mathbf{R})$ is the magnetic coupling. We use the notation $\lambda(\mathbf{q} = 0) \equiv \lambda^{\text{para}}$ (paramagnetic region) and $\lambda(\mathbf{q} = (0, 0, \frac{1}{2})) \equiv \lambda^{\text{ord}}$ (AFM ordered region); a suffix \parallel or \perp is further used to take into account anisotropic exchange. Magnetic interactions among the Ce moments in the paramagnetic region are accounted for by

$$\frac{1}{\chi_\parallel} = \frac{1}{\chi_\parallel^{CF}} - \lambda_\parallel^{\text{para}} \quad (4)$$

and

$$\frac{1}{\chi_\perp} = \frac{1}{\chi_\perp^{CF}} - \lambda_\perp^{\text{para}} \quad (5)$$

where χ_\parallel and χ_\perp are the components of the uniform susceptibility parallel and perpendicular to the c -axis, respectively. χ_\parallel^{CF} and χ_\perp^{CF} are the respective Van Vleck susceptibilities. Since the study has been performed on polycrystalline material, the total measured susceptibility follows from

$$\chi = \frac{1}{3} \chi_\parallel + \frac{2}{3} \chi_\perp. \quad (6)$$

To reduce the number of adjustable parameters for least-squares fits, we have used the crystal-field splittings previously derived from inelastic neutron scattering experiments [9]. There, one inelastic excitation was observed at 190 and 60 K for CeCu_5 and CeCu_4Al ,

respectively. Since the second inelastic excitation expected for these compounds was not observed directly from inelastic neutron scattering, ^{155}Gd Mössbauer measurement have been performed on the homologous Gd series $\text{GdCu}_{5-x}\text{Al}_x$ [10] in order to obtain the nuclear quadrupole coupling constant ΔE_Q , which is related to the crystal-field coefficient A_2^0 by [11]

$$A_2^0 = -193.8 \Delta E_Q \quad (7)$$

where A_2^0 is in K a_0^{-2} (a_0 being the Bohr radius) and ΔE_Q is given in mm s^{-1} . The values of ΔE_Q , which confirm previous measurements [12], are reported in table 1. The crystal-field parameter B_2^0 of the CF Hamiltonian for the Ce^{3+} ion is given by

$$B_2^0 = \alpha_j \langle r^2 \rangle (1 - \sigma_2) A_2^0 \quad (8)$$

where α_j is the second-order Stevens constant, $\langle r^2 \rangle$ is the second moment of the 4f radial wave function and the CF parameter A_2^0 does not depend on a particular rare earth (RE). σ_2 is a screening coefficient estimated to amount to about 0.6 for any RE atom. By taking $\alpha_j = -5.714 \times 10^{-2}$ and $\langle r^2 \rangle = 1.309$ au for Ce and $1 - \sigma_2 \approx 0.4$ for the RE series, a first approximation of B_2^0 for Ce follows from

$$B_2^0 = 5.8 \Delta E_Q \quad (9)$$

where B_2^0 is given in K.

The resulting values of B_2^0 are still subject to some uncertainty, in particular for a proper treatment of shielding effects. For CePd_2Al_3 , for which the CF parameters are better known [13], it turns out that B_2^0 obtained by the above procedure is too small by a factor of 1.7. We therefore multiply B_2^0 obtained from equation (9) by a scale factor 1.7. Using the deduced values of the splitting Δ_1 , the second CF parameter B_4^0 may be calculated using

$$B_4^0 = \frac{6B_2^0 - \Delta_1}{300} \quad (10)$$

and

$$\Delta_2 = 18B_2^0 - 60B_4^0. \quad (11)$$

Δ_1 and Δ_2 are the energy separations of the first and second excited CF levels from the ground state, respectively. Taking the experimentally observed values of Δ_1 (for CeCu_3Al_2 we use Δ_1 for CeCu_4Al since the magnetic entropy of the former matches that of the latter below about 60 K) and the values of ΔE_Q for $x = 0, 1, 2$ into account, we have evaluated B_2^0 , B_4^0 as well as Δ_2 ; these are summarized in table 1. The splitting Δ_2 for CeCu_5 is consistent with the lower bound established in reference [9]. The CF levels obtained in this way are also consistent with other thermodynamic properties like the specific heat, and the magnetic susceptibility as is shown below. The uncertainties in the determination of the CF parameters (which are often a major difficulty for quantitative studies of intermetallic RE compounds) do not preclude the possibility of studying the trends in the magnetic behaviour through the alloy series.

Some additional constraints have been taken into consideration when calculating the temperature-dependent susceptibility. It has already been shown for the antiferromagnetic structure of CeCu_5 [7] that

$$\lambda_{\perp}^{\text{para}} \simeq \frac{1}{9} \lambda_{\parallel}^{\text{ord}} - \chi_{\perp}(0)^{-1}. \quad (12)$$

$\chi_{\perp}(0)$ is the perpendicular susceptibility contribution at $T = 0$. For polycrystalline material $\chi_{\perp}(0) = \frac{3}{2} \chi_{\text{exp}}^{\text{poly}}(0)$. Additionally, $\lambda_{\parallel}^{\text{ord}} = 4k_B T_N / (g_j^2 \mu_B^2 N_A)$. Using experimental values of

CeCu₅ one finds $\lambda_{\perp}^{\text{para}} \approx 0.89 \text{ mol emu}^{-1}$. However, there is no similar relation available for $\lambda_{\parallel}^{\text{para}}$. A fit to $\chi(T)$ for CeCu₅ using the parameters B_2^0 , B_4^0 and $\lambda_{\perp}^{\text{para}}$ deduced earlier is shown as a solid line in figure 1. The only parameter allowed to vary in that case is $\lambda_{\parallel}^{\text{para}}$ (which has been found to have little effect on the average susceptibility). This description shows reasonable agreement with the experimental data. Since neither CeCu₄Al nor CeCu₃Al₂ shows long-range magnetic order, the molecular-field constants $\lambda_{\perp}^{\text{para}}$ and $\lambda_{\parallel}^{\text{para}}$ are freely adjustable in the fitting procedure. Because the number of free parameters is increased for both systems, a better agreement between the theoretical model and the experimental data can be reached (solid lines for CeCu₄Al and CeCu₃Al₂).

2.2. NCA calculations of the magnetic susceptibility

In order to study the influence of Kondo interaction on the temperature-dependent magnetic susceptibility we perform calculations applying the self-consistent large-degeneracy expansion, also known as the NCA [1, 6, 14–16]. This technique allows us to calculate finite-temperature properties of the Kondo impurity problem for realistic situations including a crystalline electric field and a magnetic field. The NCA consists in solving a set of coupled integral equations for the empty- and occupied-state propagators of the impurity state. Once the propagators are known, the magnetization and the susceptibility are calculated from the spectral densities and f-moment spectrum, respectively. The susceptibility contains Curie as well as Van Vleck terms.

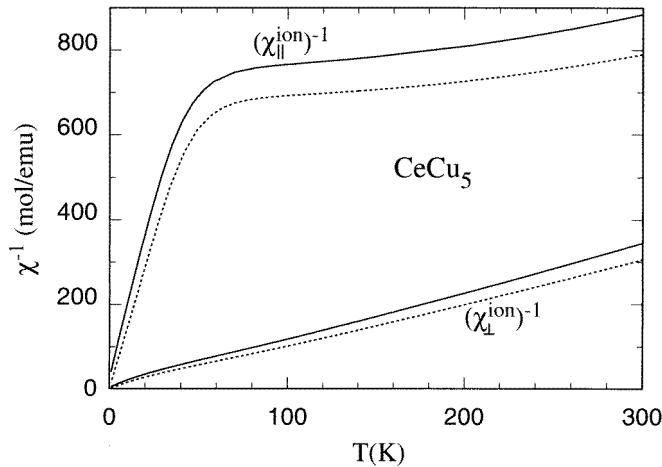


Figure 2. The inverse of the ionic susceptibility of CeCu₅ parallel and perpendicular to the *c*-axis. Dotted lines: the CF susceptibility. Solid lines: the NCA susceptibility with $T_K = 2.2 \text{ K}$.

The definition and choice of the Kondo temperature T_K must be specified. In order to keep the number of free parameters to a minimum, we assume the values of T_K determined from specific heat results and reported in table 1. Since T_K is not an input of the NCA code (the inputs are instead the *f*-level position E_f and the hybridization width Δ), the parameters of the NCA calculation are varied until the low-temperature susceptibility agrees with that previously calculated with the variational method for a given T_K [17]. An equivalent definition is to take $k_B T_K$ as the peak position in the calculated *f*-spectral function [14]: we have checked that the two definitions agree to within a factor close to unity.

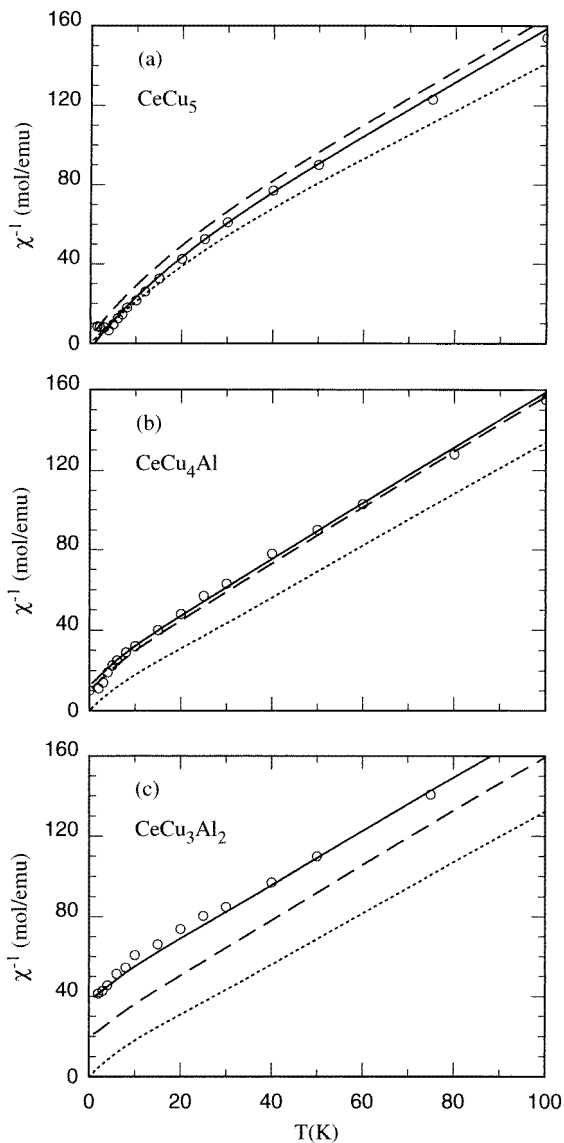


Figure 3. The inverse of the spherically averaged susceptibility of $\text{CeCu}_{5-x}\text{Al}_x$, $x = 0, 1, 2$. Dotted lines: the CF susceptibility. Dashed lines: the NCA ionic susceptibility (no molecular field). Solid lines: the NCA susceptibility with a molecular field (with the parameters given in table 1). Points: experimental values.

In figure 2 we show the inverse ionic susceptibility of CeCu_5 parallel and perpendicular to the c -axis. The susceptibility is strongly anisotropic and is much larger in the ab -plane than along the c -axis: the ratio is $\chi_{\perp}/\chi_{\parallel} \simeq 9$ for temperatures smaller than the CF splitting, and then it decreases slightly. The Kondo effect produces an upward shift of the inverse susceptibility compared to the CF-only susceptibility (dotted lines in figure 2). The shift is much larger for χ_{\parallel} as can be understood qualitatively using the approximate formula

$\chi \sim \mu^2/(T + T_K)$. The shift is then $\sim T_K/\mu^2$, which is about nine times larger for χ_{\parallel} than for χ_{\perp} . The shift increases with temperature: this derives from the fact that the physics gradually changes from that of a CF doublet to that of a sextuplet, with the effective Kondo temperature increasing accordingly. This behaviour distinguishes the shift due to the Kondo effect from that due to a molecular field, but the two effects remain difficult to separate in practice.

In figure 3 we show the inverse of the spherically averaged susceptibility for the three compounds $\text{CeCu}_{5-x}\text{Al}_x$, $x = 0, 1, 2$, compared with the experimental results. We restrict the comparison to the temperature range 0–100 K in order to display the effects associated with the CF. The dotted lines show the pure CF susceptibility, while dashed lines represent the ionic NCA susceptibility without any molecular field (the inclusion of molecular fields leading to the solid lines in figure 3 is discussed below). Comparison with the experimental data shows that a pure CF calculation is insufficient, and that the inclusion of a Kondo interaction via the NCA goes in the right direction to explain the experimental results. However, discrepancies remain which call for the inclusion of a molecular field in the paramagnetic susceptibility. A closer look at figure 3 reveals that the relevant molecular-field constant has to be positive (ferromagnetic) for CeCu_5 , very small or slightly negative for CeCu_4Al and negative (antiferromagnetic) for CeCu_3Al_2 (table 1).

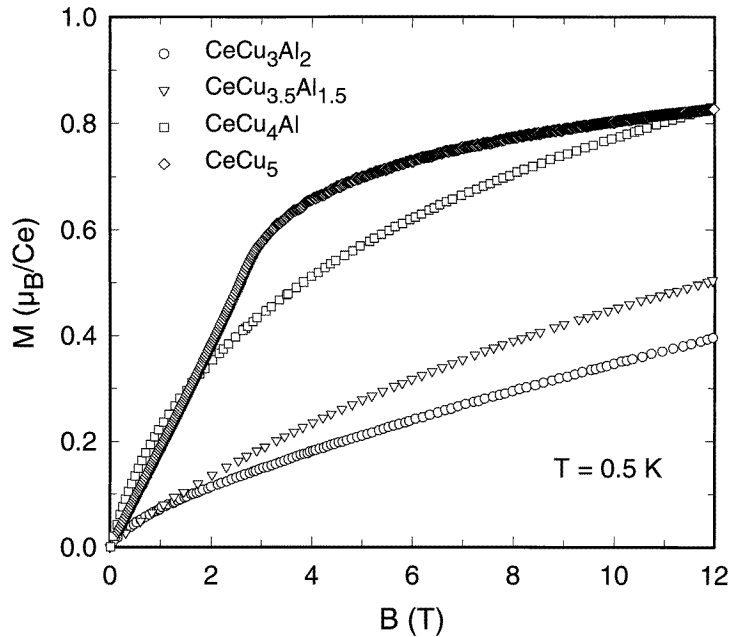


Figure 4. The isothermal magnetization of $\text{CeCu}_{5-x}\text{Al}_x$ at $T = 500$ mK.

Molecular fields in the paramagnetic region are taken into account by $(\chi_{\alpha})^{-1} = (\chi_{\alpha}^{\text{ion}})^{-1} - \lambda_{\alpha}^{\text{para}}$, $\alpha = \parallel, \perp$, where the ionic susceptibility χ^{ion} takes into account both CF and Kondo interaction. The procedure for determining the molecular-field constants $\lambda_{\parallel}^{\text{para}}$, $\lambda_{\perp}^{\text{para}}$ is also similar to that of section 2.1, but for consistency we must now employ the NCA susceptibility. For CeCu_5 , the experimental value of the Néel temperature leads to $\lambda_{\parallel}^{\text{ord}} = \chi_{\parallel}^{\text{ion}}(T_N)^{-1} = 94.9$ mol emu $^{-1}$, and applying equation (12) we get $\lambda_{\perp}^{\text{para}} = 4.24$ mol emu $^{-1}$ (we note that $\lambda_{\perp}^{\text{para}} < \lambda_{\parallel}^{\text{ord}}/9$, which implies that the system orders

antiferromagnetically). The value of $\lambda_{\parallel}^{\text{para}}$ is not determined, since the average susceptibility depends weakly on this parameter. Here we take $\lambda_{\parallel}^{\text{para}} = 0$ for simplicity and in order to reduce the number of independent parameters. For the other compounds in the series, $\lambda_{\perp}^{\text{para}}$ is determined from a best fit to the susceptibility, and $\lambda_{\parallel}^{\text{para}}$ is again taken to be equal to zero. The resulting values are reported in table 1 and the spherically averaged susceptibility is shown by solid lines in figure 3. Good agreement with the experimental data is obtained for the three compounds. The values of $\lambda_{\perp}^{\text{para}}$ so obtained from this NCA fit are quite different from those determined in section 2.1: in particular the negative values are much smaller in absolute value. $\lambda_{\perp}^{\text{para}}$ changes from ferromagnetic to antiferromagnetic on increasing the Al concentration, as anticipated. This may be related to a change of sign of the RKKY interaction on increasing the conduction electron density, or possibly to dominance of the superexchange contribution to the electronic polarization, as found in similar systems [18, 19].

3. Isothermal magnetization of $CeCu_{5-x}Al_x$

Figure 4 shows magnetization curves for $x = 0, 1, 1.5$ and 2 measured at $T = 500$ mK in fields up to 12 T. $CeCu_5$ shows a metamagnetic transition at $\mu_0 H = 2.5$ T (which can be seen more easily by plotting dM/dH versus H : see e.g. figure 6 of reference [4]), proving the ground state of this compound to be antiferromagnetic. Increasing the Al content shows that the metamagnetic behaviour vanishes and the magnetization at a given applied field is reduced. For $x = 2$ the magnetization at 12 T is just about half of that of $CeCu_5$. In terms of a Kondo compensation of the Ce moments, we can immediately conclude that the interaction strength, and therefore T_K , increases owing to the Al/Cu substitution.

The ionic magnetization of $CeCu_5$ calculated by the NCA was already shown in reference [7]; here we recall the main features. The magnetization perpendicular to the c -axis is much larger than that along the c -axis. Both of them increase steadily with the field, but while the parallel magnetization tends slowly to the constant value $0.428 \mu_B$, the perpendicular magnetization continues to increase due to Van Vleck coupling with the excited CF levels. Even at fields of 10 or 20 T, the magnetization is reduced by about 20% compared to the pure CF magnetization. Thus the magnetic moment is appreciably reduced by the Kondo effect even at relatively large values of the applied field.

For the ordered compound $CeCu_5$, the induced magnetization in the antiferromagnetic phase is calculated in molecular-field theory by solving a model with two sublattices 1 and 2 with appropriate molecular-field constants (the \parallel or \perp index is understood):

$$M_1 = M_{\text{ion}}(\lambda_{11}M_1 + \lambda_{12}M_2 + B_{\text{ext}}) \quad (13)$$

$$M_2 = M_{\text{ion}}(\lambda_{12}M_1 + \lambda_{11}M_2 + B_{\text{ext}}) \quad (14)$$

where $\lambda_{11} = (\lambda^{\text{para}} + \lambda^{\text{ord}})/2$, $\lambda_{12} = (\lambda^{\text{para}} - \lambda^{\text{ord}})/2$ and B_{ext} is the external field. The total magnetization per Ce atom is then $(M_1 + M_2)/2$. For the case of compounds showing no magnetic order, a description is achieved using a single equation.

Figure 5 shows the calculated magnetization (spherical average) of the four compounds with $x = 0, 1, 1.5, 2$. The molecular-field constants used in the calculation are those determined from a fit to the susceptibility and reported in table 1; $\lambda_{\perp}^{\text{ord}}$ for $CeCu_5$ has been taken equal to zero for simplicity. For $CeCu_{3.5}Al_{1.5}$ there are no values for the CF parameters and we therefore adopted the values for $CeCu_4Al$. In addition we assumed that $T_K = 7$ K and $\lambda_{\perp} = -10.7$ mol emu $^{-1}$ for $CeCu_{3.5}Al_{1.5}$.

For comparison, the dashed line displays the CF magnetization of $CeCu_5$, i.e., when T_K is set equal to zero. For $CeCu_5$ it can be seen that the induced magnetization is close to

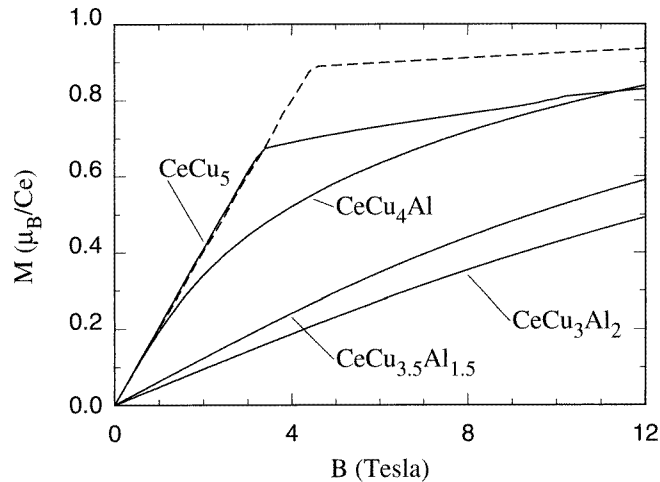


Figure 5. The self-consistent NCA magnetization of $\text{CeCu}_{5-x}\text{Al}_x$ at $T = 0.5$ K; the values of T_K and the molecular-field parameters are as in table 1. CeCu_5 : antiferromagnetic state, two-sublattice model. Other compounds: paramagnetic state. Dashed line: the self-consistent magnetization of CeCu_5 in a two-sublattice model for $T_K = 0$.

the CF value for $B < 3$ T, but shows a significant reduction for larger fields. The average magnetization is dominated by that perpendicular to the c -axis. The change of slope at around $B = 3$ T is due to the fact that the moments on the two sublattices are initially aligned along the c -axis, and then rotate into the perpendicular direction as the field is increased. The parallel magnetization is always very small, due to the large antiferromagnetic coupling, and gives a minor contribution to the spherical average. Comparison with the results of figure 4 shows good agreement and proves that the magnetic moment of CeCu_5 is indeed appreciably reduced at high fields.

The trend of the self-consistent magnetization for the other three compounds is also well reproduced by the model. The decrease of the magnetization through the series is the result of increasing T_K and also of the increased AFM values of $\lambda_{\perp}^{\text{para}}$. The calculated magnetization of CeCu_4Al shows excellent agreement with the experimental data; those for $\text{CeCu}_{3.5}\text{Al}_{1.5}$ and CeCu_3Al_2 are also in good agreement. The minor discrepancies which remain for the alloys can be attributed to the limited information about CF parameters for these compounds. We emphasize that the same set of molecular-field constants have been used to reproduce both the susceptibility and the magnetization results; thus the magnetization data can also be taken as an indication of a change of sign of $\lambda_{\perp}^{\text{para}}$ and an evolution towards more AFM values through the series.

4. Conclusions

Susceptibility and magnetization results have been presented for the hexagonal compounds $\text{CeCu}_{5-x}\text{Al}_x$. These were complemented by ^{155}Gd Mössbauer measurements on the homologous Gd series, $\text{GdCu}_{5-x}\text{Al}_x$, in order to obtain information about the CF parameters.

An analysis of the susceptibility using a CF model yields large negative values for the molecular-field constants, which are difficult to interpret. A reinterpretation of the susceptibility results on the basis of accurate NCA calculations reveals that most of the

deviation of the measured susceptibility from the CF results is explained by the presence of the Kondo effect. Smaller values for the molecular-field constants are needed; they change from ferromagnetic to antiferromagnetic on increasing the Al concentration in the series. The effect of the Kondo interaction on the susceptibility is pronounced even at high temperatures, since the effective T_K increases with temperature.

The present model provides a good description of the magnetization data for the different alloys in the series, with essentially no free parameters. For $CeCu_5$ a two-sublattice model has been solved. The Kondo temperature is sizeably increased in going from $CeCu_5$ to $CeCu_3Al_2$ and explains the quenching of the magnetic order by the Kondo effect. The magnetic moment in an external field is appreciably reduced compared to the CF values, even for values of the magnetic field energy that are much larger than the Kondo energy scale. This is a confirmation of theoretical expectations based on exact solutions of the Kondo problem [1], which are verified here for compounds where the Kondo effect, anisotropy and molecular fields all play an important role in determining the magnetic properties.

Acknowledgments

The authors are indebted to J P Sanchez and P Vulliet for performing Mössbauer measurements on $GdCu_{5-x}Al_x$. Parts of the work were supported by the Austrian FWF, project 10947, and the UK Engineering and Physical Science Research Council.

References

- [1] Hewson A C 1993 *The Kondo Problem to Heavy Fermions* (Cambridge: Cambridge University Press)
- [2] Bauer E, Gratz E and Schmitzer C 1987 *J. Magn. Magn. Mater.* **63+64** 37
- [3] Willis J O, Aiken R H, Fisk Z, Zirngibl E, Thompson J D, Ott H R and Batlogg B 1987 *Theoretical and Experimental Aspects of Valence Fluctuations and Heavy Fermions* ed L C Gupta and S K Malik (New York: Plenum) p 57
- [4] Bauer E, Rotter M, Keller L, Fischer P, Ellerby M and McEwen K 1994 *J. Phys.: Condens. Matter* **6** 5533
- [5] Bauer E 1991 *Adv. Phys.* **40** 417
- [6] Monnier R, Degiorgi L and Delley B 1990 *Phys. Rev. B* **41** 573
- [7] Amoretti G, Andreani L C, Bauer E, Delley B, Monnier R, Pavarini E and Santini P 1997 *Solid State Commun.* **103** 585
- [8] Scharper F W, Eichler A, Hallmann A and Bauer E 1996 *J. Magn. Magn. Mater.* **158** 613
- [9] Gignoux D, Schmitt D, Bauer E and Murani A 1990 *J. Magn. Magn. Mater.* **88** 63
- [10] Sanchez J P and Vulliet P 1996 private communication
- [11] Ofer S, Nowik I and Cohen S G 1968 *Chemical Applications of the Mössbauer Spectroscopy* ed V I Goldanskii and R H Herber (New York: Academic) p 427
- [12] Mulder F M, Thiel R C and Buschow K H J 1992 *J. Alloys Compounds* **190** 77
Buschow K H J, Coehoorn R, Mulder F M and Thiel R C 1993 *J. Magn. Magn. Mater.* **118** 347
- [13] Colineau E, Sanchez J P, Rebizant J and Winan J M 1994 *Solid State Commun.* **92** 915
- [14] Bickers N E, Cox D and Wilkins J W 1987 *Phys. Rev. B* **36** 2036
- [15] Bickers N E 1987 *Rev. Mod. Phys.* **59** 845
- [16] Cox D 1987 *Phys. Rev. B* **35** 4561
- [17] Andreani L C, Livioti E, Santini P and Amoretti G 1996 *Z. Phys. B* **100** 95
- [18] Hernando A, Rojo J M, Gomez-Sal J C and Novo J M 1996 *J. Appl. Phys.* **79** 4815
Garcia Soldevilla J, Gomez-Sal J C, Rodriguez-Fernandez J, Espeso J I, Monconduit L, Allemand J and Paccard D 1997 *Physica B* **230–232** 117
- [19] Pavarini E, Andreani L C and Amoretti G 1996 *Int. J. Mod. Phys. B* **10** 1167